Measuring the Stable Isotope Composition of Water in Brine from Halite Fluid Inclusions and Borehole Brine Seeps Using Cavity Ring-Down Spectroscopy

Eldridge, Daniel Lee
Mills, Melissa M.
Miller, Hayden Bryce Dutcher
Otto, Shawn
Davis, Jon Eric
Guiltinan, Eric Joseph
Rahn, Thomas A.
Kuhlman, Kristopher L.
Stauffer, Philip H.

To be published in: ACS Earth and Space Chemistry

DOI to publisher's version: 10.1021/acsearthspacechem.4c00107

ACS EARTH AND SPACE CHEMISTRY

http://pubs.acs.org/journal/aesccq

Article

Measuring the Stable Isotope Composition of Water in Brine from Halite Fluid Inclusions and Borehole Brine Seeps Using Cavity Ring-Down Spectroscopy

Daniel L. Eldridge,* Melissa M. Mills, Hayden B. D. Miller, Shawn Otto, Jon E. Davis, Eric J. Guiltinan, Thom Rahn, Kristopher L. Kuhlman, and Philip H. Stauffer

Cite This: https://doi.org/10.1021/acsearthspacechem.4c00107

Read Online

ACCESS | Metrics & More | Article Recommendations | Supporting Information

ABSTRACT: Naturally occurring bedded salt deposits are considered robust for the permanent disposal of heat-generating nuclear waste due to their unique physical and geological properties. The Brine Availability Test in Salt (BATS) is a US-DOE Office of Nuclear Energy funded project that uses heated borehole experiments underground (~655 meters depth) at the Waste Isolation Pilot Plant (WIPP) in the bedded salt deposits of the Salado Formation to investigate the capacity for safe disposal of high-level, heat generating nuclear waste in salt. Uncertainties associated with brine mobility near heat-generating waste motivates the need to characterize the processes and sources of brine in salt deposits. Intragranular halite fluid inclusions are a potential source of brine that can migrate under temperature gradients toward heat sources. We developed a methodology to measure the stable isotopic compositions of water (δD_{VSMOW}, $\delta^{18}O_{VSMOW}$) in brine from halite fluid inclusions using Cavity Ring-Down Spectroscopy that accounts for memory effects using a unique reference-sample-reference bracketing approach and that minimizes sample size requirements. We applied this approach to halite samples obtained from WIPP and compare these data to seeped brines collected from horizontal boreholes at WIPP after drilling at ambient conditions. The stable isotope compositions that we obtain for halite fluid inclusions ($\delta^{18}O_{VSMOW}$ = +3.24 ± 0.53‰, δD_{VSMOW} = −25.3 ± 5.1‰, ±1σ, n = 5) generally agree with previous measurements and likely reflect a combination of syn-depositional and/or postdepositional processes. The seep brines are isotopically distinct ($\delta^{18}O_{VSMOW}$ = +3.46 ± 0.84‰, δD_{VSMOW} = +7.3 ± 3.5‰, ±1σ, n = 35) and instead resemble evaporated seawater. We discuss our results in the context of prior WIPP-proximal waters and lay the groundwork for using stable isotopes of water in brine as a tool to assess the heat-induced mobilization of halite fluid inclusions in ongoing heating experiments that comprise the Brine Availability Test in Salt.

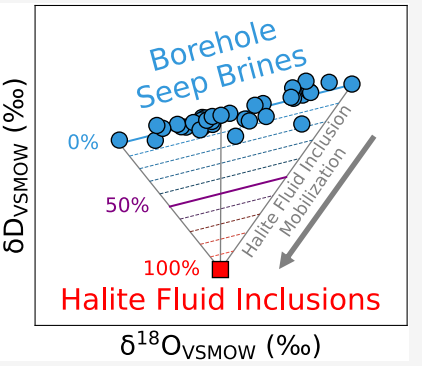

KEYWORDS: *halite fluid inclusions, brines, stable isotopes, CRDS, nuclear waste, repository science, BATS*

1. INTRODUCTION

1.1. Motivation: Brine Mobilization at the Waste Isolation Pilot Plant. The Waste Isolation Pilot Plant (WIPP) in southeastern New Mexico (Figure 1) is a U.S. DOE-Office of Environmental Management facility developed for the disposal of nonheat generating transuranic (TRU) waste in salt.[1] WIPP is hosted in Permian-aged (298.9−251.9 Ma) salt deposits of the Salado Formation in the northern Delaware Basin[2] (Figure 1). The Salado Formation is primarily (~90%) comprised of halite (NaCl) that is sporadically interbedded with 1 to 10 meter intervals of anhydrite ($CaSO_4$), polyhalite ($K_2Ca_2Mg(SO_4)_4{\cdot}2H_2O$), mudstone (mixed siliciclastic and carbonate [dominantly magnesite, $MgCO_3$]), along with localized potash deposits (McNutt Potash Zone, Figure 1).[2] The WIPP facility site (~655 meters below ground) was excavated just above a nonhalite marker bed (MB139) that contains polyhalitized anhydrite.[3] The general sedimentary sequence of the Salado Formation is interpreted to reflect the evaporation of seawater in a shallow marginal basin that was periodically flushed with fresh seawater and experienced episodes of continental deposition driven by inflow of meteoric waters.[4]

Globally, ~2.8 million m^3 of high-level heat-generating nuclear waste is in temporary storage[5] and the volume of stored waste continues to increase without a firm solution for permanent disposal. Salt deposits are considered robust for the permanent disposal of nuclear waste (either heat-generating or not) due to their low permeability, high thermal conductivity, and self-healing capability.[6−8] Salt deposits, along with other

Received: April 24, 2024
Revised: November 8, 2024
Accepted: November 13, 2024

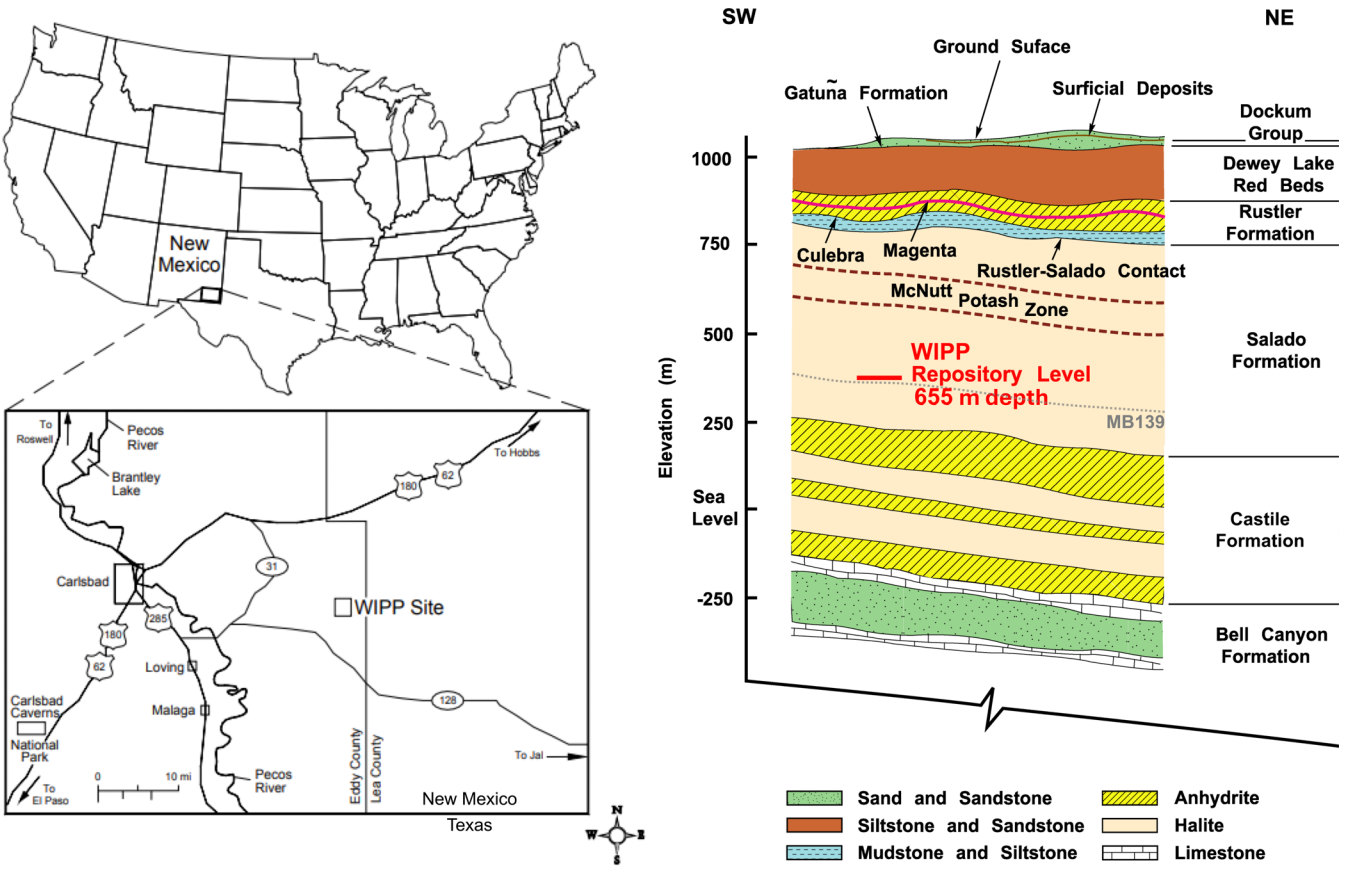

Figure 1. Location of the Waste Isolation Pilot Plant (WIPP) in New Mexico, USA. On the right, simplified stratigraphy of the WIPP site illustrating proximity to Marker Bed 139 (MB139).

rock types (crystalline and argillaceous rocks), are actively being researched for potential disposal of high-level heat-generating nuclear waste.[6,7,9]

Uncertainties associated with brine mobility near heat-generating waste motivate studies to characterize the processes and sources of brine in salt deposits to better predict the amount of brine that may ultimately reach the waste in a salt repository. For example, in salt, heat-mobilized brines can enhance the corrosion of disposal containers and waste forms, transport radionuclides, and compromise the creep closure sealing of the repository due to brine back-pressure.[10] In general, bedded salt deposits are relatively dry (on average <5 wt % H_2O) but do contain water in various forms: (i) intergranular brines that exist at grain boundaries, (ii) brines trapped in salt crystals as halite fluid inclusions (HFI), (iii) structural water in hydrous minerals, and (iv) adsorbed water in clays and other minerals.[1,11,12]

The Brine Availability Test in Salt (BATS) is a US-DOE Office of Nuclear Energy funded collaboration between Sandia, Los Alamos, and Lawrence Berkeley national laboratories that uses heated borehole experiments underground at WIPP to assess the possibility of disposing of high-level, heat generating nuclear waste in salt formations. Ongoing borehole heating experiments (BATS 2.0) at WIPP specifically seek to determine the effect of heating on the mobilization of brine in salt.[11,13,14] Halite fluid inclusions are a potential source of heat-driven brine mobilization at WIPP and in the ongoing BATS 2.0 experiments. Halite fluid inclusions have long been known to migrate in the presence of temperature gradients via a dissolution and precipitation mechanism.[12] For example, in experiments performed with single halite crystals between 108 to 260 °C and subjected to 1.5 °C/cm temperature gradients (i.e., 10^3 to 10^4 times greater than typical shallow continental geothermal gradients), halite fluid inclusions were observed to migrate at rates such that inclusions may reach grain boundaries within yearlong time scales.[12] Under these conditions, fluid inclusions migrate toward the heat source and, thus, are predicted to migrate toward heat-generating nuclear waste in a disposal scenario. We are investigating this mechanism to assess whether brine is expected to mobilize and accumulate at grain boundaries in proximity to heat-generating nuclear waste.

The hydrogen and oxygen stable isotope compositions of water have long been used to determine the origins (e.g., meteoric vs oceanic) and histories of natural waters.[15−23] We hypothesize that stable isotopes of various waters in the salt deposits surrounding WIPP will yield insight into the origins and potential mobilization processes of brine in the BATS 2.0 experiments.[11,13,14] As a first step to assess this possibility, we have characterized the stable isotope composition of water in brine from both halite fluid inclusions and horizontal borehole brine seeps. We have developed a new method to determine the stable isotope compositions of water in brine within halite fluid inclusions that is based on a distinct measurement design that is tailored to fluid inclusion analysis using Cavity Ring-Down Spectroscopy (CRDS). Our method accounts for memory effects based on single measurements of small samples (~200 nL of water). We compare these measurements to those of evolved brines from boreholes during baseline nonheating events as part of the ongoing BATS 2.0

https://doi.org/10.1021/acsearthspacechem.4c00107
ACS Earth Space Chem. XXXX, XXX, XXX−XXX

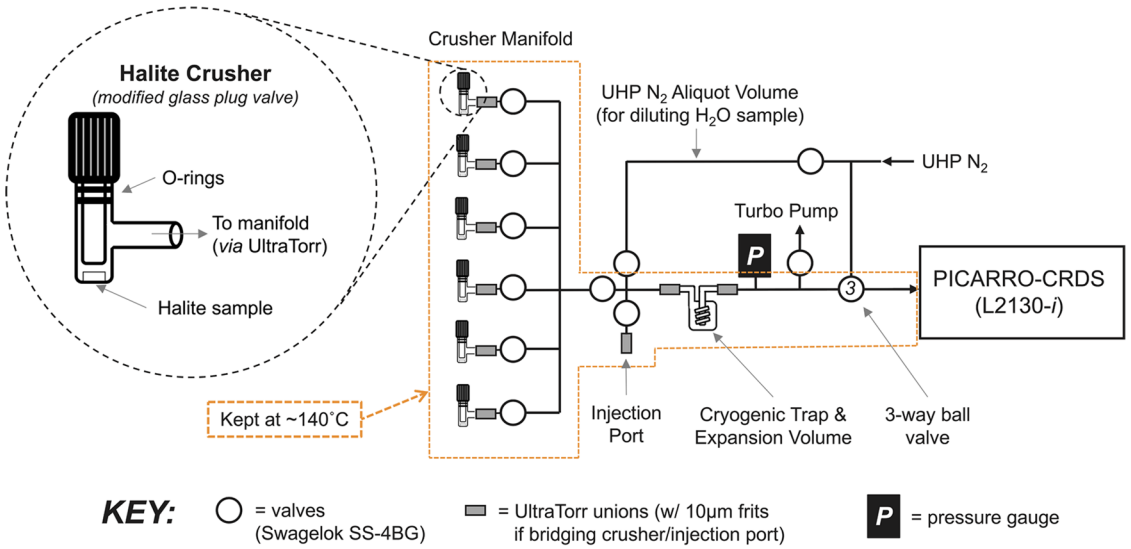

Figure 2. Schematic drawing of the vacuum line system used to liberate water from brine in halite fluid inclusions based on the design of ref 32. The area bounded by the orange dashed line indicates the components that are heated (~140 °C).

experiments.[11,13,14] We aim to develop a framework to detect halite fluid inclusions that have been mobilized by heat using stable isotope measurements. Additionally, we compare our results to prior stable isotope measurements of halite fluid inclusions and various waters in proximity to WIPP.[3,24,25]

1.2. CRDS Methodologies to Measure Water in Fluid Inclusions: Memory Effects. CRDS instruments greatly simplify stable isotope measurements of water by allowing analysis to be performed directly on water analytes without equilibrations and/or chemical conversions to other gaseous analytes such as H_2 and CO_2, which are routine for Isotope Ratio Mass Spectrometry (IRMS) measurements.[18,26,27] However, memory effects are associated with the stable isotope measurement of vaporized liquid water samples handled in vacuum systems[26] and are well-documented in CRDS systems for H_2O analytes.[28−31] Memory effects are the result of contamination of given water sample measurements by prior sample analysis. Commonly, memory effects are circumvented in CRDS systems by repeat measurements of the same sample, eliminating the memory effect by dilution (or "conditioning"). The multi-injection or conditioning method is effective for waters where sample size is not limiting and multiple injections of the same sample are possible. However, this approach is often not possible for fluid inclusion samples because repeat measurements of the same fluid inclusion are not typically feasible due to their small size and the practical challenge of subsampling the same fluid inclusion for repeat measurements.

A number of other approaches have been developed to account for memory effects[28−31] that either have or can be applied to fluid inclusion analysis using CRDS. We summarize some of the more common approaches as follows: (1) A method that involves the determination of "memory coefficients" (parameterized herein as χ) based on mass balance modeling and using water standards of known and different isotopic compositions that are used to correct measured isotope compositions of identically treated unknowns;[28,31−33] (2) A preconditioning method whereby waters with similar isotopic composition to the fluid inclusions are injected several times prior to the measurement of a fluid inclusion sample;[34] and (3) A moisturized carrier gas method (rather than standard dry gas) where all sample measurements are made in the presence of a known/characterizable water vapor background.[35−38] Attempts have also been made to construct more detailed physical models of memory effects that involve multiple contamination sources with varying rates of isotope exchange among them that can be applied to injected samples.[30] Any given approach for circumventing or characterizing memory effects has advantages and disadvantages where the methodology of choice may depend on the specific application.

In this study, we developed and tested an approach that accounts for memory effects in the measurement of water from halite fluid inclusion brines, which builds upon prior CRDS approaches but follows a distinct measurement design of reference-sample-reference bracketing. Like prior approaches, ours is based on a simple application of mass balance equations to account for memory effects. However, we derive equations that allow for the determination of memory-corrected isotopic compositions of a sample based only on the measured (and known) reference water composition and the memory-affected compositions (i.e., without the need to explicitly determine and apply memory coefficients). The primary assumption in our derivation is that memory coefficients are constant between measurements,[29,32] which is a calculable output of our approach and advantageously allows for monitoring of memory coefficients within and between measurement sessions. Another advantage of this approach is that it does not require repeat measurements of unknowns and therefore utilizes an overall smaller sample size. The disadvantages of this approach include: (i) the requirement that water amounts obtained from a crushed sample be equivalent to injected reference water (difficult to determine/judge beforehand, especially for brines in halite fluid inclusions containing unknown or variable dissolved salt contents), and (ii) relatively low sample throughput if the specific approach outlined here is followed (~3 sample unknowns per day if no check standards are run).

2. METHODS

2.1. Liberation of Water from Halite Fluid Inclusions (HFI). Following a previous design,[32] we constructed a vacuum

https://doi.org/10.1021/acsearthspacechem.4c00107
ACS Earth Space Chem. XXXX, XXX, XXX−XXX

line to crush halite and vacuum volatilize HFI water at a moderate temperature (~140 °C) to prepare for stable isotope measurement using CRDS (Figure 2). This system is referred to as the "halite crush line" in subsequent descriptions. The vacuum line is comprised of the following components connected via manifold with 0.25 in. OD electropolished Swagelok tubing: (1) water sample inlet with two methods of introducing sample (halite crushers and injection port); (2) a ~50 mL borosilicate glass cryogenic trap and expansion volume (custom-made to the specifications of a previous design;[32] Quark Glass, Vineland, NJ) connected to the manifold via UltraTorr fittings; (3) a valved volume used to aliquot Ultra High Purity (UHP) N_2 (99.999%; Airgas) for dilutions; and (4) a 3-way ball valve that directs gas flow to a Picarro CRDS from either a UHP N_2 tank (background mode, no sample measurement) or a sample in the vacuum line (sample measurement mode). The two methods for water sample inlet are (a) halite crushing devices made from modified borosilicate glass plug valves (Chemglass Life Sciences; custom-modified by Quark Glass, Vineland, NJ) connected to the manifold via UltraTorr fittings equipped with 10 μm stainless steel filter frits (VICI-Valco; frits prevent salt buildup in the vacuum line), and: (b) syringe needle injection port (VICI-Valco) comprised of septa connected to the manifold also via UltraTorr fittings equipped with 10 μm filter frits. The vacuum line was wrapped in heat tape and kept at ~140 °C and the temperature monitored using K-type thermocouples.

The procedure for preparing a given sample (either injected reference water or crushed halite) is as follows. First, the 50 mL cryogenic trap and expansion volume was submerged in liquid nitrogen (LN_2) and allowed to equilibrate (~2 min). Next, a water sample was introduced (~200 nL) either by injection via syringe or crushing halite and allowed to equilibrate with the LN_2 trap (5 min). The trap volume was then isolated and the LN_2 replaced with a jacketed resistance heater to thermally equilibrate to ~140 °C (~5 min). The water vapor pressure was recorded and water was refrozen in the trap with LN_2 (5 min). Aliquots of UHP N_2 were then added to the frozen water sample to achieve a final dilution of ~2.5 to 3%. The LN_2 was again swapped with the jacketed resistance heater to thermally equilibrate the gas mixture (~140 °C). The sample was then introduced to the Picarro water isotope analyzer using the 3-way ball valve (Figure 2). The total time for this procedure is approximately 40 to 50 min including CRDS measurement time.

A uniform ~200 nL of water (~11 μmoles) was used for any given water measurement using the halite crush line. For waters obtained from HFI, this volume of water was not directly determined. Instead, the water amount was determined to be comparable to known injected water amounts based on the measured pressure of recovered water from a crushed sample.

2.2. Stable Isotope Measurements (Cavity Ring-Down Spectroscopy). Stable isotope measurements were performed on a Picarro L2130-*i* Cavity Ring-Down Spectroscopy (CRDS) analyzer capable of simultaneous measurement of hydrogen (δD_{VSMOW}) and oxygen ($\delta^{18}O_{VSMOW}$) isotope compositions of water vapor. Stable isotope compositions of water from the halite crush line were determined by averaging data ±30 s from the water peak maximum (Figure S1) and applied uniformly to all halite crush line measurements (samples and standards) via a Python script. Isotope compositions were calculated relative to the Vienna Standard Mean Ocean Water (VSMOW) international reference standard based on measurements of USGS standards (described below) using conventional δ-notation in units of parts per thousand (‰)

$$\delta D_{VSMOW} = \left(\frac{{}^{D}R_{sample}}{{}^{D}R_{VSMOW}} - 1 \right) \times 1000 \quad (1)$$

$$\delta^{18}O_{VSMOW} = \left(\frac{{}^{18}R_{sample}}{{}^{18}R_{VSMOW}} - 1 \right) \times 1000 \quad (2)$$

Here, R refers to an isotope ratio: ${}^{D}R$ = D/H (=^{2}H/^{1}H) and ${}^{18}R$ = ^{18}O/^{16}O.

Measurements of two USGS calibration standards on our halite crush line were used to standardize our isotopic measurements of halite fluid inclusions and in house standards (i.e., two-point calibration). These USGS standards were also used to calibrate our measurements of borehole seep brines that were measured using a Picarro autosampler and vaporization module (described in Section 2.5). The isotopic compositions of the USGS standards span the range of our in-house standards and include USGS48 (δD_{VSMOW} = −2.0 ± 0.4‰, $\delta^{18}O_{VSMOW}$ = −2.224 ± 0.012‰)[39] and USGS47 (δD_{VSMOW} = −150.2 ± 0.5‰, $\delta^{18}O_{VSMOW}$ = −19.80 ± 0.02‰).[40] Memory effects associated with our measurements of USGS47 and USGS48 on the halite crush line were circumvented using the multiple injection approach (Section 2.3). Five injections and measurements are sufficient to obtain injection-invariant isotope values using the halite crush line (i.e., injections 1−4 are thrown out and injections ≥5 are used). Our in-house standard waters (Standard 1 and Standard 2) were measured in every measurement session on the halite crush line by both the multiple injection and bracketing approach (Section 2.3) to monitor for long-term drift (Section 3.2), determine reproducibility of our method, and correct for memory effects using our measurement design (Section 2.3).

2.3. Measurement Design of HFI to Account for Memory Effects. We developed a distinct reference-sample-reference bracketing measurement design to account for memory effects tailored to fluid inclusion sample measurement on our halite crush line. This approach accounts for memory effects using only measured memory-affected isotopic compositions and the known/measured isotopic composition of a reference water. Our measurement design incorporates the same mass balance treatment and definition of memory coefficients as prior work.[28,31−33] The bracketing measurement design allows us to derive an equation with only one unknown (i.e., the memory-corrected sample isotope composition). Prior measurement designs using similar principles and assumptions generate two unknowns (i.e., both the memory coefficient and the memory-corrected sample isotope composition). Thus, for our design, the bracketing approach eliminates the need to determine memory coefficients for data correction. Instead, memory coefficients can be calculated from the data as outputs and be used for monitoring.

Our measurement sequence follows the pattern: reference (×5 to achieve injection-invariant values), sample, reference, sample, reference (etc.) where each sample measurement is bracketed by a measurement of the reference water. The initial reference water injections condition the vacuum line and CRDS for mass balance modeling that allows for the

https://doi.org/10.1021/acsearthspacechem.4c00107
ACS Earth Space Chem. XXXX, XXX, XXX−XXX

calculation of memory-corrected values for the subsequent bracketed samples.

The equations for memory-corrected values were derived using mass balance equations and assuming the memory coefficient is constant between injections. For the first bracketed sample measurement, the memory-corrected isotope ratio is given by

$$R_{s(1),true} = [(R_{s(1),meas})^2 - R_{s(1),meas}R_{ref,true} - R_{+1ref,meas}R_{ref,true} + (R_{ref,true})^2]/[R_{s(1),meas} - R_{+1ref,meas}] \quad (3)$$

The memory-corrected isotope ratio of the subsequent bracketed sample measurements ($n \geq 1$) is given by

$$R_{s(n+1),true} = [R_{s(n+1),meas}R_{ref,true} - (R_{s(n+1),meas})^2 + R_{+1ref,meas}R_{-1ref,meas} - R_{-1ref,meas}R_{ref,true}]/[R_{+1ref,meas} - R_{s,meas}] \quad (4)$$

In both equations, the isotope ratio, R, can refer to either hydrogen or oxygen. Subscript "s(1)" refers to bracketed sample 1 (i.e., first bracketed sample), "s(n + 1)" refers to subsequent bracketed samples ($n \geq 1$), and "ref" refers to the reference water. Subscript "meas" refers to measured value (memory-affected) and "true" refers to the true or memory-corrected value. The "+1ref" refers to the reference water measured after the sample and "−1ref" refers to the reference water measured prior to the sample.

The assumption that memory coefficients are constant between measurements requires water amounts used in each measurement be equivalent (i.e., the amount of water extracted from a given crushed halite sample must match the amount of the reference waters). This can make fluid inclusion measurements challenging due to their heterogeneous distribution in salt. Thus, fluid inclusion samples were selected from colocated halite fragments (1 cm scale) and crushed in sequence until optimal water volumes were obtained. Importantly, we assume that our water extractions from halite fluid inclusions are complete and that no isotopic fractionation is associated with any incomplete extractions (beyond the corrections for Mg content that we discuss in Sections 2.6, 3.4, and 4.1). The ability to independently quantify the amount of inclusion fluid water in samples prior to a destructive measurement would be advantageous for calculating extraction yields and for the further application of this method.

We can calculate memory coefficients for each measurement as a check on our assumption that they are constant between measurements. The memory coefficient (χ) for any given bracketed sample measurement is given by

$$\chi_s = \frac{R_{+1ref,meas} - R_{ref,true}}{R_{s,meas} - R_{ref,true}} \quad (5)$$

Here, "s" generically refers to "sample" because the memory coefficient equation is the same regardless of bracketed sample number in the measurement sequence. Thus, memory coefficients are outputs of our measurement design. Although we did not find evidence for this in measurements presented in this work (described in Section 3.2), anomalously high or low memory coefficients may provide evidence for an errant or suspect measurement.

2.4. Halite Samples from the Waste Isolation Pilot Plant (WIPP). We applied our measurement methodology to five sets of coarsely crystalline halite fragments that contained visible fluid inclusions. Images of select fragments are provided in the Supporting Information (Figure S2). Three sets of halite fragments were obtained from hand samples of clear to gray and coarsely grained halite obtained from Waste Isolation Pilot Plant (WIPP) facility depth (655 meters depth from ground surface). Two sets of halite fragments were obtained from a recovered drill core at approximately 13.6 meters below WIPP facility depth (668.6 meters depth from ground surface; drill core SDI-BH-00004). Drill core SDI-BH-00004 was drilled 50.6 ft (15.4 meters) vertically down from WIPP facility depth in January 2014 using an Atlas Copco Diamec 264 and air as the drilling fluid. Segments of recovered rock core (3.75 in. [~9.53 cm] diameter) from drilling were preserved in heat-sealed cellophane. Marker Bed 139 (MB139; Figure 1) was reportedly encountered 3.5 ft (1.07 meters) beneath WIPP facility depth in SDI-BH-00004, with a thickness of 2.35 ft (0.72 meters), and comprised of orange-brown to gray anhydrite (laminar at base) and underlain by a horizon of clay. The section of core targeted for HFI sampling (conducted 2022) was ~1.6 ft (0.49 meters) from the base of a 16.4 ft (~5 meter) section of clear to medium gray and coarsely grained halite containing (visually) <1% polyhalite and <1 to 3% clays. This section of halite is bound above by a 0.25 ft (7.6 cm) horizon of microcrystalline anhydrite (light to medium gray) and underlain by a 4.3 ft (1.31 meter) sequence of clear to reddish-orange and coarsely crystalline polyhalitic halite.

2.5. Evolved Borehole Brines from BATS 2.0 Experiments at WIPP. In this work, we have collected and analyzed brines accumulated in BATS 2.0 horizontal boreholes during preheating phases of the experiment (i.e., "natural" seepage postdrilling). An image and schematic of the BATS 2.0 borehole array is provided in the Supporting Information (Figure S3). The BATS 2.0 horizontal boreholes were drilled using only air as the drilling fluid and therefore minimize the potential for sample contamination by a drilling fluid (i.e., no additional water or organics were added to the system in the process of drilling). Brines were sampled from BATS 2.0 boreholes by either sponge (n = 31 samples; sterile dehydrated Speci-Sponge packaged in a Whirl-Pak bag; Nasco) or vacuum pump (n = 4 samples). Prior to measurement, aliquots of each brine sample (~0.5 mL) were filtered using 0.45 μm nylon spin filters (MP Biomedicals, LLC). Stable isotope measurements of BATS 2.0 borehole brines were performed using the same Picarro L2130-*i* water isotope analyzer described above but equipped with a vaporization module (Picarro Model A0211) and autosampler (Picarro Model A0325) and fed with dry compressed air. Stainless steel salt filters on the vaporization module capture precipitated salts upon brine vaporization. VSMOW standardization was achieved using the same USGS standards described above (Section 2.2), however, measured using the Picarro autosampler and vaporization modules. The raw data processing routines were equivalent for brines and standards and performed using the Picarro software. Memory effects were circumvented using the multiple injection approach whereby 10 injections and measurements of each brine or standard were performed and only injections ≥5 were averaged.

The sponge sampling method was tested for analytical artifacts in the laboratory using high purity water (18 MΩ × cm) and brines prepared from this water and anhydrous NaCl and $MgCl_2$ salts (described below). Aliquots (~10 mL) of either high purity water or prepared chloride brine were absorbed in the sponge, wrung out into a glass Petri dish cover,

https://doi.org/10.1021/acsearthspacechem.4c00107
ACS Earth Space Chem. XXXX, XXX, XXX−XXX

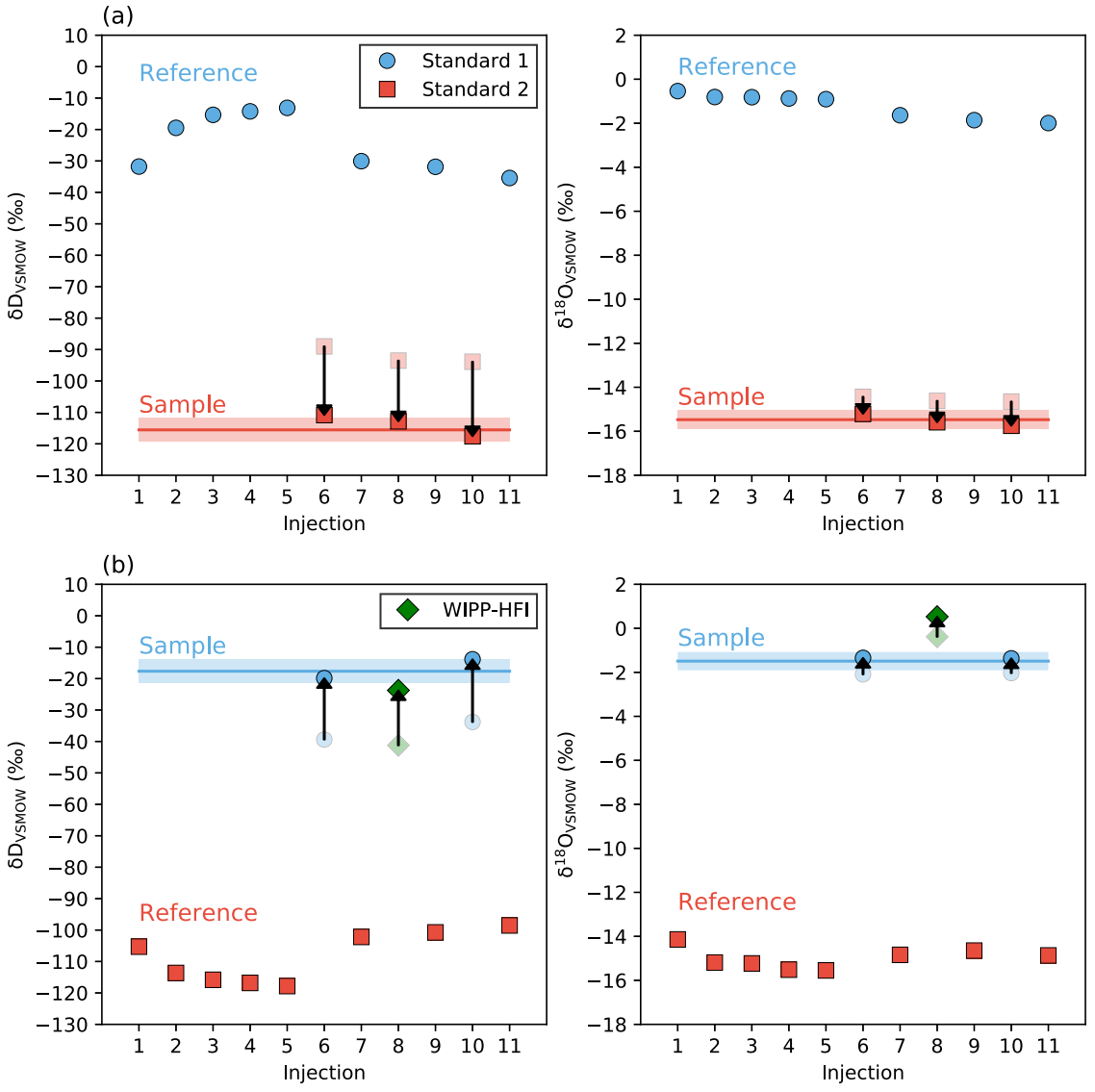

Figure 3. Illustrative examples of the bracketing measurement design developed in this study to account for memory effects in the measurement of halite fluid inclusions using the system shown in Figure 2. (a) A representative test using in-house standards (Standard 1, Standard 2) illustrating three determinations of Standard 2 using Standard 1 as the reference. (b) Similar demonstration showing the bracketed measurement of Standard 1 and a halite fluid inclusion sample using Standard 2 as the reference. In both illustrations, blue circles indicate measurements of Standard 1 that is used in (a) as a Reference and in (b) as a Sample. Similarly, red squares indicate measurements of Standard 2 that is used in (a) as a Sample and in (b) as a Reference. The transparent Sample symbols represent values uncorrected for memory effects and the vertical arrows indicate the corrections for memory effects based on eqs 3 and 4. The horizontal lines and shaded regions represent the mean and standard deviation of the mean values ($\pm 1\sigma$), respectively, of these in-house standards. The illustrations in (a, b) demonstrate that our bracketing methodology reproduces the true values of in-house standards when treated as Samples.

and immediately transferred to a borosilicate sample vial. Aliquots (~0.5 mL) of these waters were then filtered and analyzed as described above for the horizontal borehole brine seep samples.

For major solute concentration analyses, the acquired borehole brines were filtered through a 0.2 μm syringe filter to remove any solids. For ion chromatography (IC) (Dionex Aquion) analysis of major anionic species (Cl^-, Br^-, SO_4^{2-}), the filtered brine was diluted in volumetric flasks to a factor of 10^4 with deionized (DI) water. For cationic species (Ca^{2+}, K^+, Li^+, Mg^{2+}, Na^+) and boron, an Inductively Coupled Plasma Optical Emission Spectrometer (ICP-OES) (PerkinElmer Optima 8000) was used and brine is diluted by factors of 100 and 1000 with 2% HNO_3 to accommodate both low and high element concentrations. Instruments were calibrated with respective standards made from Dionex 7-Anion for IC and Spex CertiPrep Quality Control Standard 23 for ICP during the time of analysis. All instrument calibrations were evaluated to ensure linear fits to be $R^2 > 0.999$ for every element. Samples were diluted and analyzed for respective element concentration ranges adequate for each instrument (i.e., <100 ppm).

2.6. Sensitivity Tests with Chloride Brines (Na^+, K^+, Ca^{2+}, Mg^{2+}). The vacuum volatilization of water from brine could be accompanied by isotopic fractionation due to the precipitation of salts (e.g., hydrous salts). We performed a sensitivity test for this possibility by injecting and measuring brines prepared from the chloride salts of the four major cations in seawater: Na^+, K^+, Ca^{2+}, and Mg^{2+}. Brines were prepared from the same batch of high purity water (18 MΩ ×

https://doi.org/10.1021/acsearthspacechem.4c00107
ACS Earth Space Chem. XXXX, XXX, XXX−XXX

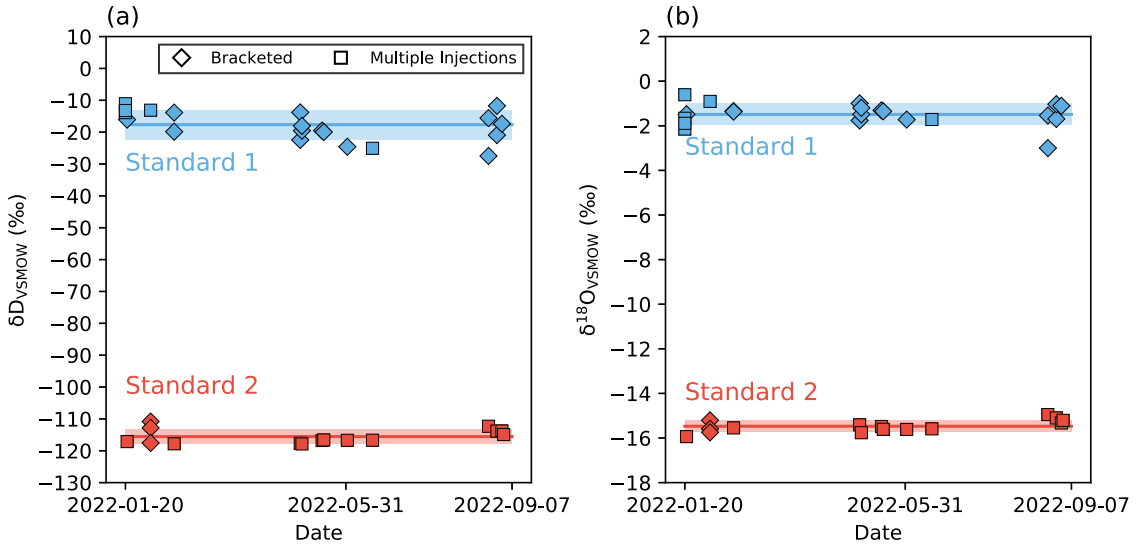

Figure 4. Long-term reproducibility of in-house standards (Standard 1, Standard 2) using both the multiple-injection (squares) and bracketing approaches (diamonds). All measurements were performed using the system illustrated in Figure 2. (a) δD_{VSMOW}, (b) $\delta^{18}O_{VSMOW}$. The illustrated time period includes all halite fluid inclusion measurements presented in this study. The horizontal lines and shaded regions represent mean and standard deviation of the mean values ($\pm 1\sigma$), respectively, for each in house standard.

cm) and using anhydrous salts up to concentrations of 4.97 to 5.23 m (m = mol/kg H_2O): NaCl (Sigma-Aldrich), KCl (Sigma-Aldrich), $CaCl_2$ (Sigma-Aldrich), and $MgCl_2$ (Research Products International). The dissolution of anhydrous $MgCl_2$ and $CaCl_2$ (highly exothermic reactions) was carried out stepwise by dissolving small portions of salt at a time while keeping the solution chilled during dissolution (but not frozen) aided by liquid nitrogen.[41] For tests using the halite crushing vacuum line (pertinent to the HFI measurements), brines were measured using our bracketing approach where the high purity water (no salts added) was used as the reference and brines treated as samples. For tests using the Picarro autosampler and vaporization module, prepared chloride brines and the high purity water (no salts added) were measured using the multi-injection approach. Fractionations associated with the vacuum volatilization of brine were quantified as the measured isotopic composition of the Cl-brine vs the high purity water from which the Cl-brine was prepared (no salts added) using conventional α-notation:

$$ {}^{D}\alpha_{\text{brine/pure}} = \frac{(\delta D_{\text{brine}}/1000 + 1)}{(\delta D_{\text{pure}}/1000 + 1)} \quad (6) $$

$$ {}^{18}\alpha_{\text{brine/pure}} = \frac{(\delta^{18}O_{\text{brine}}/1000 + 1)}{(\delta^{18}O_{\text{pure}}/1000 + 1)} \quad (7) $$

3. RESULTS

3.1. Tests of the Bracketing Approach. Reference waters (in-house standards) of different isotopic composition were used to test the newly developed mass balance bracketing approach that accounts for memory effects (one test illustrated in Figure 3a). Here, the in-house Standard 1 (δD_{VSMOW} = −17.7 ± 4.6‰ and $\delta^{18}O_{VSMOW}$ = −1.49 ± 0.49‰, all 1σ; see Section 3.2) was used as a reference water and the in-house Standard 2 (δD_{VSMOW} = −115.6 ± 2.2‰ and $\delta^{18}O_{VSMOW}$ = −15.47 ± 0.26‰, all 1σ; see Section 3.2) was used as the sample. The transparent data points represent the memory-affected, uncorrected values and represent shifts in δD from true values by +22 to +27‰ and shifts in $\delta^{18}O$ +0.8 to +1.1‰. The corrected values (applying eqs 3−4) yield δD_{VSMOW} and $\delta^{18}O_{VSMOW}$ values for Standard 2 that are within 1 to 2σ of their nominal values based on long-term reproducibility (Section 3.2).

In Figure 3b, we illustrate a measurement sequence that included a WIPP-HFI sample measurement. Here, the in-house Standard 2 was used as the reference and the in-house Standard 1 was measured using the bracketing method both before and after the WIPP-HFI sample. The corrected values for Standard 1 yield δD_{VSMOW} and $\delta^{18}O_{VSMOW}$ values that are within 1σ of their nominal values based on long-term reproducibility (Section 3.2). Standard 2 was used as the reference for all WIPP-HFI measurements reported in this study and each bracketed measurement of a WIPP-HFI sample in this study was preceded by a bracketed measurement of Standard 1.

3.2. Long-Term Reproducibility of δD, $\delta^{18}O$, and Memory Coefficients (χ). Measurements of our in-house standard waters (Standard 1, Standard 2) over the period of HFI measurements are summarized in Figure 4. Both Standard 1 and Standard 2 were measured by the multiple injection and the bracketing method presented here. Standard 2 was chosen as a reference water for the HFI measurements due to the large difference in its isotopic composition from the HFI samples, and as a result was mostly measured by the multiple injection method. Standard 1 has an isotopic composition closer to the HFI samples and was measured with every HFI sample as a check standard using the bracketing method (Figure 3b). Together, these measurements of Standard 1 and Standard 2 indicate a long-term reproducibility of ±3.8‰ for δD and ±0.42‰ for $\delta^{18}O$ (1σ). No evidence of significant drift was found in measured values of our in-house standards over the time period of measurements (Figure 4).

Long-term measurements of memory coefficients (outputs of measurement design; eq 5) are presented in Figure 5, which include data from both bracketed in-house standards and HFI measurements. The mean memory coefficient (χ) for δD is 0.25 ± 0.03 and for $\delta^{18}O$ is 0.07 ± 0.02 (1σ). The memory

https://doi.org/10.1021/acsearthspacechem.4c00107
ACS Earth Space Chem. XXXX, XXX, XXX−XXX

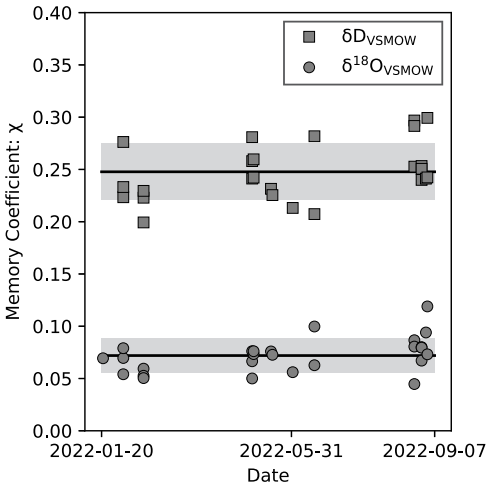

Figure 5. Long-term reproducibility of memory coefficients for δD_{VSMOW} (squares) and $\delta^{18}O_{VSMOW}$ (circles) measurements. Time period corresponds to Figure 4. The horizontal lines and shaded gray regions represent mean and standard deviation of the mean values ($\pm 1\sigma$), respectively.

coefficient for δD is significantly higher than that for $\delta^{18}O$ by a factor of ~3.5×, which is comparable to the results of prior studies.[31,32] Significant trends in the memory coefficients with time are not apparent, indicating they are likely constant within and between measurement sessions for the constant amount of water used for each measurement (200 nL).

3.3. WIPP HFI. The results of our new WIPP HFI measurements are provided in Table 1. The δD_{VSMOW} of the five measurements range between −15.9 to −29.7‰, with a mean value of δD_{VSMOW} = −25.3 ± 5.1‰ (1σ). The error is comparable to, but slightly higher than, the long-term reproducibility based on the repeat measurements of in-house standards (±3.8‰, 1σ). The $\delta^{18}O_{VSMOW}$ range from 0.53 to 2.11‰ and a mean value of $\delta^{18}O_{VSMOW}$ = +1.44 ± 0.53‰ (1σ) when not corrected for Mg content (discussed in Sections 3.4 and 4.1), which yields an error that is also comparable to our long-term reproducibility (±0.42‰, 1σ). Note that values for $\delta^{18}O_{VSMOW}$ reported in Table 1 include the small correction for Mg content that is discussed below (Sections 3.4 and 4.1). No observable trend is found in either δD_{VSMOW} or $\delta^{18}O_{VSMOW}$ as a function of depth over the narrow range of sampled depths (655 to 669 m).

3.4. Tests of Precipitation Effects with Injected Chloride Brines of Cations Na^+, K^+, Mg^{2+}, and Ca^{2+}. The results of our sensitivity test performed with injected brines on the halite crush line (pertinent to HFI measurements) are presented in Figure S4. The concentration of measured brines was: 4.97 *m* NaCl, 4.91 *m* KCl, 0.99 to 5.32 *m* $CaCl_2$, and 1.08 to 4.96 *m* $MgCl_2$ (*m* = moles salt per kg of H_2O). We did not observe any significant δD fractionation (parametrized as ${}^{D}\alpha_{brine/pure}$) associated with the vacuum volatilization of the measured brines (Figure S4a). Each determination of ${}^{D}\alpha_{brine/pure}$ is within $\pm 1\sigma$ of no fractionation based on the propagated long-term reproducibility of our measurements. This is also the case for $\delta^{18}O$ fractionations (${}^{18}\alpha_{brine/pure}$) with the exception of $MgCl_2$ brines, which we found to be associated with significant fractionations (Figure S4b). Values of $({}^{18}\alpha_{brine/pure} - 1) \times 1000$ computed for $MgCl_2$ brines vary systematically with concentration from −1.9‰ at 1.08 *m* to −5.8‰ at 4.96 *m*. If these data are linearly fit with a 0‰ intercept (i.e., no fractionation at a $MgCl_2$ concentration of 0 *m*), the relationship suggests a −1.24 ± 0.11‰ (1 s.e.) fractionation (brine vs pure) per 1 *m* of $MgCl_2$ (not shown). In practical terms, accounting for this analytical artifact would thus require the addition of approximately +1.24‰ to a memory-corrected $\delta^{18}O$ value per 1 *m* of $MgCl_2$ in the vacuum volatilized aqueous fluid. Section 4.1 describes the potential impact of this analytical artifact on measured $\delta^{18}O_{VSMOW}$ values given previously reported solute concentrations in WIPP-proximal HFI.

Comparable tests performed using the Picarro autosampler and vaporization module (pertinent to the BATS 2.0 borehole brine measurements) obtain very similar results to the halite crush line. First, no significant fractionation was registered in values of δD or $\delta^{18}O$ using the sponge sampling method vs no sponge for the waters tested: high purity water, 5.06 m NaCl, and 0.98 and 2.47 m $MgCl_2$ (Figure S5). Similar to the results of the halite crush line, no significant fractionation is observed for the vaporization of brines using the Picarro vaporizer (Figure S5) except with respect to $\delta^{18}O$ values of vaporized $MgCl_2$ brines (Figure S5b). A correction of +1.14 to $\delta^{18}O$ (±0.13, 1 s.e.) per 1 m of $MgCl_2$ in the vaporized fluid is obtained (including the sponge test results), which is indistinguishable from the correction obtained from the halite crush line (+1.24 ± 0.11‰ per 1 *m* $MgCl_2$). Thus, we find no evidence for artifacts associated with the sponge sampling of brines but do find evidence to correct horizontal borehole brine seep $\delta^{18}O$ values for their Mg content (discussed in Sections 4.1 and 4.2).

Table 1. Results of Halite Fluid Inclusion (HFI) Measurements Using the Halite Crush Line and Methodology Presented Here[a]

analysis date	sample name	depth (m)	mass (mg)	measurement type	inlet *T* (°C)	% H_2O	H_2O (ppm)	χ ($\delta^{18}O$)	χ (δD)	$\delta^{18}O_{VSMOW}$ (‰)[b]	δD_{VSMOW} (‰)
2/18/22	WIPP halite facility depth (A)	655.00	690.0	bracketed	142	2.6	11,858	0.059	0.223	2.33	−23.74
5/4/22	WIPP halite facility depth (B)	655.00	573.8	bracketed	140	2.5	10,036	0.076	0.281	3.47	−28.75
6/16/22	WIPP halite facility depth (C)	655.00	632.8	bracketed	140	2.6	10,426	0.100	0.282	3.46	−28.45
8/24/22	SDI-BH-00004 (A)	668.64	125.9	bracketed	140	2.2	9923	0.087	0.297	3.04	−29.69
8/29/22	SDI-BH-00004 (B)	668.64	194.2	bracketed	140	2.5	11,628	0.080	0.251	3.91	−15.89

[a]Note that % H_2O refers to manometric measurements performed on the halite crush line and H_2O (ppm) refers to the value on the Picarro; these water contents will not necessarily directly correspond due to additional dilution with UHP N_2 during sample inlet. [b]Mg-corrected using a correction factor of +1.80‰ as described in the text.

https://doi.org/10.1021/acsearthspacechem.4c00107
ACS Earth Space Chem. XXXX, XXX, XXX−XXX

3.5. Evolved Brines from BATS 2.0 Boreholes. BATS 2.0 borehole brines obtained from the preheating phase (n = 35; Table 2) range in δD_{VSMOW} from +1.8 to +14.1‰ (mean +6.9 ± 3.5‰, 1σ) and range in $\delta^{18}O_{VSMOW}$ between +0.39 to +3.83‰ (mean = +2.06 ± 0.83‰, 1σ) when uncorrected for Mg content (note: $\delta^{18}O_{VSMOW}$ values in Table 2 include this correction that is discussed in Section 4.2). Measurements of USGS standards described above using the Picarro autosampler and vaporization module during BATS 2.0 borehole brine measurement campaigns indicate a long-term reproducibility of ±2.3‰ for δD_{VSMOW} and ±0.40‰ for $\delta^{18}O_{VSMOW}$ (±1σ).

Table 2. Stable Isotope Compositions of BATS 2.0 Borehole Brines Collected in the Pre-Heating Phase of the Experiment[a]

borehole	collection date	sampling method	$\delta^{18}O_{VSMOW}$ (‰)[b]	δD_{VSMOW} (‰)
AE1	2/2/22	sponge	2.28	1.76
AE3	2/2/22	sponge	2.99	4.61
E2	2/2/22	sponge	2.73	4.53
E3	2/2/22	sponge	2.66	4.60
F1	2/2/22	sponge	2.97	6.55
T1	2/2/22	sponge	1.75	1.81
AE4	2/24/22	sponge	3.12	5.09
D	2/24/22	sponge	3.02	6.45
E2	2/24/22	sponge	2.61	5.10
E3	2/24/22	sponge	2.97	6.02
F2	2/24/22	sponge	2.39	4.27
SM	2/24/22	sponge	2.84	5.48
AE2	3/8/22	sponge	3.60	6.21
AE4	3/8/22	sponge	4.46	11.24
D	3/8/22	sponge	4.55	12.05
E1	3/8/22	sponge	3.87	9.46
E2	3/8/22	sponge	4.85	13.91
E3	3/8/22	sponge	3.38	7.42
E4	3/8/22	sponge	4.32	10.57
F1	3/8/22	sponge	4.57	11.79
F2	3/8/22	sponge	2.94	3.96
HP	3/8/22	sponge	4.51	14.14
SL	3/8/22	sponge	4.31	12.74
SM	3/8/22	sponge	3.75	9.10
T1	3/8/22	sponge	3.11	5.72
AE3	3/22/22	sponge	3.92	6.75
AE4	3/22/22	sponge	4.29	10.77
D	3/22/22	sponge	3.67	5.82
F1	3/22/22	sponge	5.18	13.54
F2	3/22/22	sponge	3.46	2.61
SM	3/22/22	sponge	4.44	5.18
HSM	5/3/22	vacuum-pump	3.04	5.96
HSM	5/31/22	vacuum-pump	3.12	6.75
HSM	6/13/22	vacuum-pump	3.25	7.01
HSM	7/11/22	vacuum-pump	2.30	4.87

[a]For a picture and schematic of the borehole array, please see the Supporting Materials. [b]Mg-corrected using a correction factor of +1.35‰ as described in the text.

4. DISCUSSION

4.1. WIPP HFI: Impact of Brine Composition on Measured Stable Isotope Compositions. Using our methodology, we observe that measured $\delta^{18}O$ compositions are affected by the presence of Mg^{2+} but are not affected by the presence of the other major cations of seawater over the investigated concentrations. We were not able to measure the concentrations of solutes in halite fluid inclusion brines as part of our study. Instead, we use literature data to assess the potential impact of this issue on our oxygen isotope measurements. A prior study[42] determined major solute concentrations of brines in 111 HFI at WIPP reported to be from 645 meters depth. The most abundant cations in these HFI samples are Na^+ (range of 0.57 to 4.8 m) and Mg^{2+} (range of 0.53 to 3.34 m). The other major cations are in significantly lower abundance (i.e., K^+ range of 0.03 to 0.49 m; $Ca^{2+} \leq 0.06$ m). Cl^- is by far the most abundant anion (4.3 to 10.3 m) followed by SO_4^{2-} (0.07 to 0.43 m). Another prior study[43] provided major solute concentrations of brines in 31 halite fluid inclusion samples from the WIPP drill core ERDA-9[44] corresponding to depths of 655 to 670.6 meters that are broadly similar: Na^+ = 1.05 to 5.34 m, Mg^{2+} = 0.835 to 3.340 m, K^+ = 0.08 to 0.56 m, and $Ca^{2+} \approx 0.02$ m (detected in only 3 of 31 samples). As above, Cl^- is by far the most abundant anion (5.6 to 7.7 m) followed by SO_4^{2-} (0.14 to 0.46 m).

In Figure S6, we summarize the Mg^{2+} concentrations of WIPP HFI from prior work.[42,43] The mean concentration of Mg^{2+} in these HFI samples is 1.45 ± 0.53 m (1σ, n = 142). Based on the empirical relationship from our $MgCl_2$ test (Figure S4b and Section 3.3), this mean Mg^{2+} concentration applied uniformly to our HFI measurements results in a correction of +1.80‰ to our measured $\delta^{18}O$ values. Thus, values of $\delta^{18}O_{VSMOW}$ corrected for vacuum volatilization in this way range between 2.33 to 3.91‰ (Table 1) and yield a mean value of $\delta^{18}O_{VSMOW}$ = 3.24 ± 0.53‰ (1σ; n = 5). In the following, we will discuss and visualize the data that includes this Mg-correction.

4.2. BATS 2.0 Borehole Brines: Impact of Mg^{2+} on Measured Stable Isotope Compositions. For the 35 BATS 2.0 borehole brines analyzed (preheating phase of experiment), we obtain a mean Mg^{2+} concentration of 1.07 ± 0.11 mol/L. Accounting for the difference in concentration units (mol/kg H_2O in our tests vs mol/L measured for borehole brines), applying this Mg concentration uniformly to our BATS 2.0 brine data results in a correction of +1.35‰ to BATS 2.0 borehole $\delta^{18}O_{VSMOW}$ values. In the following, we will discuss and visualize the data that includes this Mg-correction (see Table 2).

4.3. WIPP HFI: Comparisons to Previous Constraints on HFI and Other Waters in Proximity to WIPP. Figure 6 illustrates the new Waste Isolation Pilot Plant (WIPP) halite fluid inclusion (HFI) measurements in the context of prior stable isotope work performed on waters in proximity to WIPP. This includes measurements performed on shallow ground waters located in (or stratigraphically above) the Rustler Formation (27 to 209 meters depth),[25] brines collected from the base of the Salado Formation (826 meters depth),[25] brine seeps from potash mines in the Salado Formation (326 meters depth),[3] prior WIPP boreholes (~655 meters depth),[3] and HFI from samples collected at WIPP facility depth (~655 meters)[24] and drill core ERDA-9 (~628 to 631 meters, ~795 to 823 meters depths).[25] All compiled data included in Figure 6 (including metadata) are provided in the Supporting Information.

Our new stable isotope measurements of water in WIPP HFI compare well to literature values. Prior stable isotope measurements of water in HFI at or in proximity to WIPP yield values of $\delta^{18}O_{VSMOW}$ = 3.48 ± 0.68‰ at 655 m (1σ, n =

https://doi.org/10.1021/acsearthspacechem.4c00107
ACS Earth Space Chem. XXXX, XXX, XXX−XXX

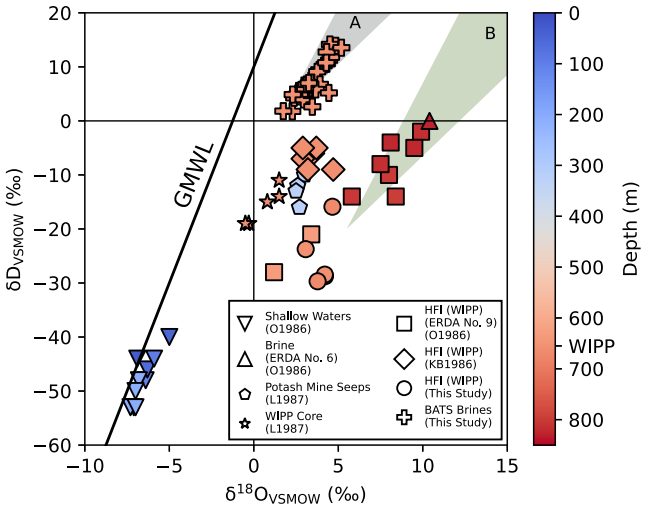

Figure 6. Summary of stable isotope determinations of waters found in proximity to the Waste Isolation Pilot Plant (WIPP) in the Delaware Basin, New Mexico. Symbols indicate the sampling types and colors refer to collection depths. The new data presented in this study are the circles (new halite fluid inclusion measurements) and crosses (BATS 2.0 horizontal borehole seep brines). GMWL = Global Meteoric Water Line. Shaded area A represents a prediction field based on a simple evaporation model described in the text. Shaded area B represents a prediction field based on this evaporation model and the incorporation of water into gypsum via precipitation (using the nominal equilibrium mother water/gypsum fractionation factor).[53] Shaded area B illustrates the original observation made by O'Neil and co-workers[25] that the water in ERDA No. 9 brine (upward pointing triangle) is consistent with having originated from the quantitative dehydration of gypsum that originally formed in isotopic equilibrium with evaporating seawater. Reference key: O1986,[25] L1987,[3] and KB1986.[24]

6)[24] and $\delta^{18}O_{VSMOW}$ = 2.3 ± 1.56‰ at 627.6 to 631.1 m (1σ, n = 2).[25] Our new WIPP HFI $\delta^{18}O_{VSMOW}$ measurements (655 to 669 m) are comparable to these values whether or not we apply the Mg^{2+} correction for vacuum volatilization: $\delta^{18}O_{VSMOW}$ = 3.24‰ with the correction and 1.44‰ without the correction [±0.53‰, 1σ, n = 5] (Section 4.1). Our new mean value that includes the Mg^{2+} correction is within 1σ of the mean values from these two prior studies. Furthermore, O'Neil and co-workers[25] obtain δD_{VSMOW} = −24.5 ± 4.9‰ (1σ, n = 2), which is indistinguishable from our measurements (i.e., mean δD_{VSMOW} = −25.3 ± 5.1‰, 1σ, n = 5) despite the tens of meter differences in sampling depths. However, both our and their[25] measurements yield significantly lower values of δD_{VSMOW} for HFI water than that obtained from Knauth and Beeunas:[24] δD_{VSMOW} = −6.8 ± 1.8‰ (1σ, n = 6). We utilized a similar crushing and vacuum volatilization method to O'Neil and co-workers[25] to liberate water from HFI (conducted at ∼140 °C in the current study vs 350 °C in O'Neil and co-workers).[25] In contrast, Knauth and Beeunas[24] utilized a higher temperature method (∼800 °C) to release water from HFI conducted at or near the melting point of halite. O'Neil and co-workers[25] stated that analytical artifacts are associated with the 800 °C method but did not provide enough information to evaluate this possibility in further detail.

We will now briefly discuss our new HFI results in the context of previous stable isotope measurements of various waters found in proximity to WIPP.[3,24,25] First, shallow ground waters and brines (≤210 m depth) found in the Rustler Formation and above units (stratigraphically above the Salado Formation; Figure 1) appear to primarily reflect a meteoric origin: $\delta^{18}O_{VSMOW}$ = −7.9 to −5‰ and δD_{VSMOW} = −55 to −40‰ (Figure 6).[25] In contrast, brine located below the WIPP site (ERDA-6; ∼826 m depth) at the contact between the Salado and Castile Formations (Figure 1) has a distinct isotopic composition ($\delta^{18}O_{VSMOW}$ = +10.4‰, δD_{VSMOW} = 0‰; Figure 6).[25] The water in this brine is consistent with having evolved from the coupled syn-depositional processes of seawater evaporation and the precipitation of gypsum (see shaded field B in Figure 6 modeled following O'Neil and co-workers).[25] In this context, the water in the ERDA-6 brine (826 m depth) is interpreted to have evolved from the dehydration of gypsum to form anhydrite and obtained its dissolved salt content by water-rock (nominally halite) reactions. Unlike HFI solute compositions,[42,43] the ERDA-6 brine (826m depth) is indeed comprised primarily of Na^+ and Cl^-.[45]

Intriguingly, data from prior work[24,25] and the current study indicate that water in brine from HFI in proximity to WIPP facility depth (∼655 m) and deeper (i.e., approaching the base of the Salado Formation)[25] have isotopic compositions that broadly fall between the aforementioned meteoric waters near the surface and the ERDA-6 brine at 826m depth (Figure 6). O'Neil and co-workers[25] suggested the possibility that the water in HFI brines fall along a binary mixing line between the near surface meteoric waters and the deeper brine of ERDA-6. This interpretation implies the possibility that meteoric waters having isotopic compositions similar to modern shallow groundwaters in the region have infiltrated the salt deposits in proximity to WIPP, mixed with deep brine, and the subsequent fluid mixture has become incorporated into HFI presumably by the recrystallization of the halite. This interpretation is broadly consistent with the apparent trend of HFI isotopic compositions with depth (Figure 6) over the relatively narrow depths sampled by O'Neil and co-workers.[25] An issue with this interpretation is that existing constraints on the major solute compositions of HFI indicate that these waters have more complex dissolved solute compositions than what might be expected by the mixing of ERDA-6 brine with meteoric waters, and have previously been interpreted to be linked to Permian seawater via a combination of evaporation and/or water-rock reactions.[42,43] This interpretation also appears to require that significant recrystallization of halite has occurred, possibly in relatively recent geologic history given the implied involvement of shallow meteoric ground waters that are currently found in the basin.

Textural criteria have been used to distinguish between primary and secondary halite crystallization and associated fluid inclusions in evaporite deposits. For example, bedded chevron salt having cubic planes of inclusions are believed to be primary crystallization features in bedded salt, which have been described locally in the Salado formation in proximity to WIPP.[12] Coarse, clear, and singular crystals of halite (with or without fluid inclusions) are often considered postdepositional and secondary crystallization features (generally of unknown but later timing), which are also present in the Salado formation in proximity to WIPP.[12,46] The latter describes the salt fragments sampled for HFI water isotope analyses in the present study.

The extent and timing of halite recrystallization in the Salado formation is not well understood. Geochronological evidence has been used to suggest that (at least locally)

https://doi.org/10.1021/acsearthspacechem.4c00107
ACS Earth Space Chem. XXXX, XXX, XXX−XXX

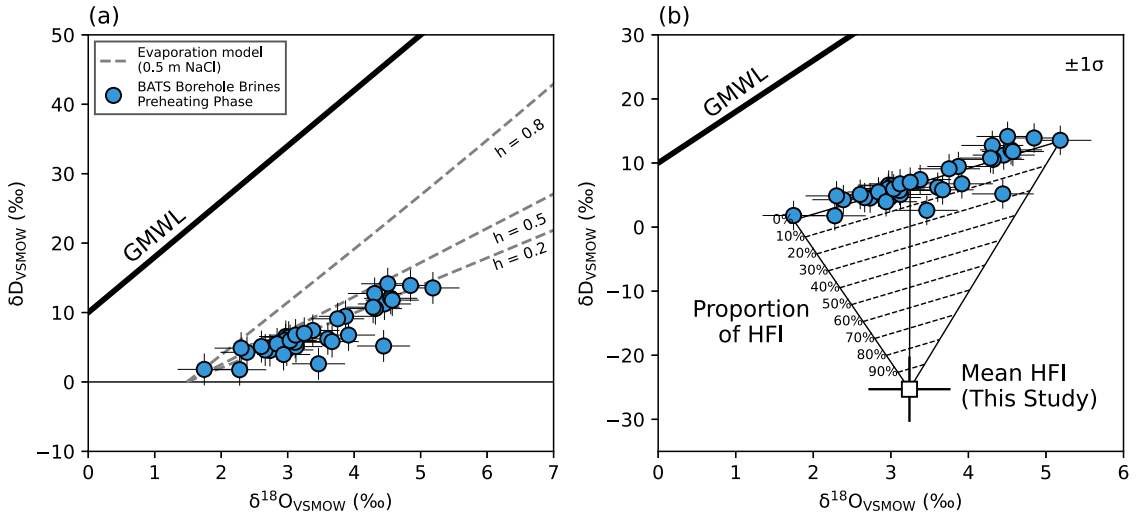

Figure 7. Comparison of borehole seep brines collected as part of the Brine Availability Test in Salt (BATS 2.0) to (a) a simple NaCl evaporation model as a function of relative humidity (described in the text and implemented after ref 50) and (b) mean values of halite fluid inclusion (HFI) measurements of this study. The triangular field in panel (b) is a mixing model between the array of BATS 2.0 borehole brine data and the mean HFI data from this study. Error bars on BATS 2.0 borehole brine data (blue circles) are $\pm 1\sigma$ and are based on the reproducibility of standards during brine measurement sessions. The error bars on the mean HFI data point (white square) represent the standard deviation of the mean of all HFI measurements ($n = 5$). We propose that the mixing model in (b) can potentially be used to quantify the proportions of HFI mobilized during ongoing BATS 2.0 heating experiments assuming no isotopic fractionation is associated with fluid inclusion migration in salt (discussed in the main text; data from heating phases of BATS 2.0 will be included in a follow-up manuscript).

primary salt minerals dating to approximately 250 Ma are preserved in the Salado Formation.[47,48] For example, Rb−Sr dating of clay minerals within the Salado formation yield ages of 254 ± 5 Ma.[47] Langbeinite ($K_2Mg_2(SO_4)_3$) from the McNutt Potash Zone yield radiometric ages based on $^{40}Ar/^{39}Ar$ methods of 251.1 ± 0.2 Ma.[48] Together, these constraints may date the depositional age of the Salado formation,[47,48] which would appear to be in proximity to the nominal Permian-Triassic boundary (251.902 ± 0.024 Ma).[49] Additional measurements based on K−Ar, $^{40}Ar/^{39}Ar$, and Rb−Sr methods applied to Salado formation salt minerals (e.g., langbeinite, sylvite, polyhalite, leonite, kieserite) record younger ages (e.g., 245 Ma;[48] clusters of ages of 216 to 174 Ma;[2] and ∼94 Ma).[48] These younger ages either indicate the lack of closure of daughter products in the interrogated minerals or provide an age of recrystallization of those minerals.[48] Thus, it appears that extant geochronology constraints neither preclude nor necessarily indicate substantial halite recrystallization or fluid inclusion mobilization in the Salado formation.[48]

Alternative interpretations to O'Neil and co-workers[25] binary mixing hypothesis have been proposed that suggest the HFI water isotope compositions are the result of both evaporative processes and variable mineral-fluid interactions including isotope exchange occurring during either deposition or later.[3,45] It is unknown which oxygen- and hydrogen-bearing minerals would be responsible for the proposed isotope exchange and exactly how waters affected by these exchange processes became preserved as fluid inclusions in halite. It appears hypothetically possible that these processes may have occurred during the deposition of the Salado Formation based on prior interpretations of sedimentary sequences.[4] It is also possible that the hypothesized meteoric water contributions to HFI in the Salado formation proposed by O'Neil and co-workers[25] were ancient and any apparent relationship to shallow meteoric ground waters found in the basin today is coincidental. Both meteoric and oceanic waters are thought to have flushed the evaporites during their deposition, and notably the isotopic compositions of the ancient meteoric waters are unknown. It thus remains unclear what exact histories/processes are reflected in the halite fluid inclusion water isotope measurements from the Salado Formation.[24,25] Below, we discuss our new measurements of BATS 2.0 borehole brines that may add additional constraints on the system.

4.4. Implications for Ongoing BATS Experiments. The BATS 2.0 brines have comparable $\delta^{18}O_{VSMOW}$ values to HFI but have δD_{VSMOW} values that differ from HFI by approximately +25 to +40‰ (Figure 6). It is difficult to explain this isotopic difference by a singular process that would directly relate the two waters. Thus, for the remainder of this discussion, we will assume that the BATS 2.0 brines are tapping into a source of brine that is distinct from nominal HFI and that both record distinct histories. The exact source or fraction from different sources of these brines in the bedded salt is currently unknown. One simple hypothesis is that they represent brine trapped at grain boundaries that has seeped from the salt along those boundaries and toward areas of damage in the bedded salt.

Unlike any other WIPP-proximal waters studied to date (to our knowledge), the BATS 2.0 borehole brines appear to isotopically resemble evaporatively evolved seawater. In Figure 7a, we compare the trend of the BATS 2.0 borehole brine data to a simple evaporation model as a function of relative humidity (h), which yields different evolution slopes in $\delta^{18}O_{VSMOW}$ vs δD_{VSMOW} space. The evaporation model is formulated after Gonfiantini and co-workers[50] and assumes a starting solution comprised of 0.5 m NaCl (roughly comparable to modern seawater, but ignoring all other solutes), accounts for associated salt effects,[51] and assumes starting isotopic compositions of δD_{VSMOW} = 0‰ and $\delta^{18}O_{VSMOW}$ = +1.5‰. The latter initial isotopic compositions

https://doi.org/10.1021/acsearthspacechem.4c00107
ACS Earth Space Chem. XXXX, XXX, XXX−XXX

of the evaporating water in the model are arbitrarily chosen but are consistent with modern seawater, which on average is nominally $\delta D_{VSMOW} = 0‰$ and $\delta^{18}O_{VSMOW} = 0‰$ but can vary spatially and temporally by a few parts per thousand depending on, for example, geographic location (relating to deep and shallow ocean circulation patterns and associated physical processes) and the extent of continental ice sheets.

Thus, we tentatively propose that the water in the BATS 2.0 borehole brines could be isotopically linked to evaporatively evolved Permian seawater. This interpretation is tentative because it may also have to be squared with the solute compositions of the brines, which are ongoing investigations. In Figure 8, we plot the measured Na^+/Cl^- vs K^+/Mg^{2+} of the

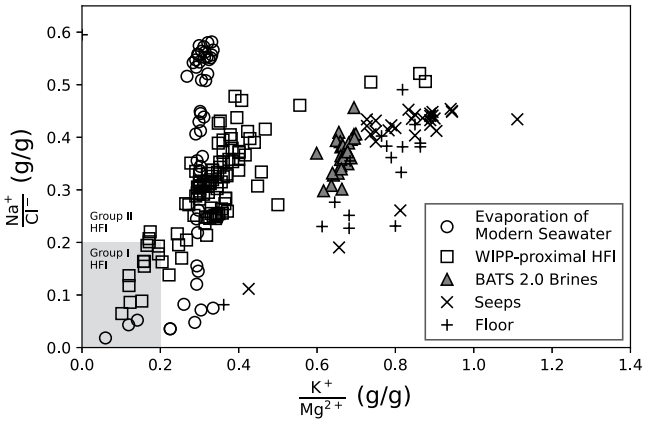

Figure 8. Major cation and anion plot comparing measurements of halite fluid inclusions (HFI) obtained in proximity to the Waste Isolation Pilot Plant (WIPP; $n = 110$),[42,43] weeps ($n = 29$) and floor brines ($n = 18$),[42] borehole seep brines obtained from the Brine Availability Test in Salt experiments (BATS 2.0; this study, $n = 32$), and data from evaporation experiments performed with modern seawater ($n = 49$).[52] The Group I and II HFI groupings are defined by ref 42.

BATS 2.0 brines and compare to prior brine measurements.[42] The Na^+/Cl^- values are comparable to previous WIPP-proximal HFI data[42,43] and evaporatively evolved modern seawater,[52] but generally have significantly higher K^+/Mg^{2+} values with few exceptions (Figure 8). The higher K^+/Mg^{2+} values for a given Na^+/Cl^- may have resulted from various diagenetic mineral/fluid reactions (e.g., involving magnesite and/or polyhalite).[42] If such hypothesized reactions do not involve the incorporation of water from hydrous minerals to the evolved brines and/or exchange of oxygen or hydrogen isotopes between waters and minerals, the isotopic compositions of the BATS 2.0 brines could primarily reflect evaporation processes even though major solutes record more complex histories. A better understanding of these reactions and their potential isotopic systematics would allow for clearer interpretation of stable isotope data from both HFI and BATS 2.0 borehole brines.

A major hypothesis that motivates the BATS 2.0 experiments is that HFI may be mobilized during heating and lead to brine accumulation in damaged salt near the heat source (i.e., high-level heat generating nuclear waste in a repository scenario). In Figure 7b, we explore a simple mixing exercise where we visualize the hypothesis that BATS 2.0 borehole brines evolved from heating (and beyond) could represent mixtures of brines collected during the preheating phases (whatever their source) and mobilized HFI. Here, the BATS 2.0 borehole brines collected during the preheating phase of BATS 2.0 are treated as one potential brine source end-member (as an array of data) and an average of our new HFI measurements (singular point) is treated as another. We assume that the BATS 2.0 borehole brines and HFI represent distinct brine reservoirs in the bedded salt, which is supported by their distinct isotopic compositions and major solute compositions (Figure 8). In this very simple framework, we expect a decrease in evolved fluid δD_{VSMOW} with increasing contributions from mobilized HFI with little to no change in $\delta^{18}O_{VSMOW}$.

The simple mixing exercise in Figure 7b assumes no significant isotopic fractionation associated with the heat-induced mobilization of HFI. Any such fractionations are not well understood or constrained to our knowledge. The nominal mechanism of HFI mobilization in thermal gradients is a combination of dissolution at the warm ends of the inclusion and precipitation at the cool ends.[12] It would seem that in order for isotopic fractionation to accompany the movement of HFI in temperature gradients, that either oxygen or hydrogen bearing salts are dissolved/precipitated during mobilization. The precipitation of hydrous salts at isotopic equilibrium is generally known to be associated with both D/H and $^{18}O/^{16}O$ isotope effects.[53,54] Thus, the evolution of δD_{VSMOW} and $\delta^{18}O_{VSMOW}$ is expected (and predictable depending on the salt mineral) if fluid inclusion mobilization involves precipitation of hydrous salts at isotopic equilibrium. Such salts would precipitate within halite crystals and would be chemically and possibly visually distinct and, thus, if identified could provide additional textural evidence of fluid inclusion mobilization. Ongoing and future heating tests will allow us to evaluate whether we see evidence of fluid inclusion mobilization using this framework, which will be described in future work.

5. SUMMARY AND CONCLUSIONS

We presented a method to determine the stable isotopic composition of water (~200 nL) in brine in halite fluid inclusions (HFI). We applied this method to the analysis of HFI from halite samples of the Salado Formation collected at the Waste Isolation Pilot Plant (WIPP) in southeastern New Mexico. The samples included coarsely grained halite from facility-depth hand samples and facility depth-proximal drill core samples from below Marker Bed 139 (MB139). Our stable isotope measurements of water in HFI are consistent with the measurements of HFI collected from halite samples of drill core ERDA-9 at comparable depths by O'Neil and co-workers.[25] We compared these results to measurements of borehole brines collected during the preheating phases of the Brine Availability Test in Salt 2.0 (BATS 2.0) conducted at WIPP, which represent "naturally" seeping brines from damaged salt under ambient conditions. The stable isotope compositions of the BATS 2.0 borehole brines are distinct (particularly δD_{VSMOW}) from our new HFI measurements. The major solute compositions of the BATS 2.0 borehole brines are also distinct from WIPP-proximal HFI from the literature. It appears likely that both the major solute and water stable isotope compositions of WIPP-proximal HFI in the Salado Formation reflect differing combinations of processes that at least include seawater evaporation and water-rock reactions, but the timing, extent, and exact details of these processes are not well understood. We propose that the data provided herein

https://doi.org/10.1021/acsearthspacechem.4c00107
ACS Earth Space Chem. XXXX, XXX, XXX−XXX

provide a simple framework to evaluate whether halite fluid inclusions are mobilized during the heating of salt (e.g., by heat-generating nuclear waste in a repository scenario) using the stable isotopic composition of evolved brines from forthcoming heating experiments of BATS 2.0.

■ ASSOCIATED CONTENT

Supporting Information

The Supporting Information is available free of charge at https://pubs.acs.org/doi/10.1021/acsearthspacechem.4c00107.

Raw Picarro data processing on the halite crush line (Figure S1); images of halite samples (Figure S2); the BATS 2.0 borehole array (Figure S3); the vacuum volatilization test with chloride brines performed on the halite crush line (Figure S4); the vacuum volatilization test with chloride brines performed on a Picarro autosampler and vaporization module (Figure S5); the histogram of literature magnesium concentrations of WIPP-proximal halite fluid inclusions (Figure S6); in-house and USGS standard data from the halite crush line (Table S1); solute concentration data for BATS 2.0 borehole seep brines (Table S2) (PDF)

Stable isotope analyses of WIPP-proximal waters compiled from the literature and illustrated in Figure 6 (XLSX)

■ AUTHOR INFORMATION

Corresponding Author

Daniel L. Eldridge − *Earth and Environmental Sciences Division, Los Alamos National Laboratory, Los Alamos, New Mexico 87545, United States;* orcid.org/0000-0001-7340-0652; Email: danieleldridge@lanl.gov

Authors

Melissa M. Mills − *Nuclear Waste Disposal Research & Analysis, Sandia National Laboratories, Albuquerque, New Mexico 87185, United States*

Hayden B. D. Miller − *Earth and Environmental Sciences Division, Los Alamos National Laboratory, Los Alamos, New Mexico 87545, United States; Chemistry Division, Los Alamos National Laboratory, Los Alamos, New Mexico 87545, United States*

Shawn Otto − *Los Alamos National Laboratory, Carlsbad Field Office, Carlsbad, New Mexico 88220, United States*

Jon E. Davis − *Los Alamos National Laboratory, Carlsbad Field Office, Carlsbad, New Mexico 88220, United States*

Eric J. Guiltinan − *Earth and Environmental Sciences Division, Los Alamos National Laboratory, Los Alamos, New Mexico 87545, United States*

Thom Rahn − *Earth and Environmental Sciences Division, Los Alamos National Laboratory, Los Alamos, New Mexico 87545, United States*

Kristopher L. Kuhlman − *Nuclear Waste Disposal Research & Analysis, Sandia National Laboratories, Albuquerque, New Mexico 87185, United States;* orcid.org/0000-0003-3397-3653

Philip H. Stauffer − *Earth and Environmental Sciences Division, Los Alamos National Laboratory, Los Alamos, New Mexico 87545, United States*

Complete contact information is available at: https://pubs.acs.org/10.1021/acsearthspacechem.4c00107

Notes

The authors declare no competing financial interest.

■ ACKNOWLEDGMENTS

The authors thank the U.S. Department of Energy Office of Nuclear Energy Spent Fuel and Waste Science and Technology campaign for funding the research under the disposal research program. This paper describes objective technical results and analysis. Any subjective views or opinions that might be expressed in the paper do not necessarily represent the views of the U.S. Department of Energy or the United States Government. This article has been coauthored by an employee of National Technology & Engineering Solutions of Sandia, LLC under Contract No. DE-NA0003525 with the U.S. Department of Energy (DOE). The employee owns all right, title and interest in and to the article and is solely responsible for its contents. The United States Government retains and the publisher, by accepting the article for publication, acknowledges that the United States Government retains a nonexclusive, paid-up, irrevocable, worldwide license to publish or reproduce the published form of this article or allow others to do so, for United States Government purposes. The DOE will provide public access to these results of federally sponsored research in accordance with the DOE Public Access Plan https://www.energy.gov/downloads/doe-public-access-plan.

■ REFERENCES

(1) Larson, K. W. Development of the Conceptual Models for Chemical Conditions and Hydrology Used in the 1996 Performance Assessment for the Waste Isolation Pilot Plant. *Reliab. Eng. Syst. Saf.* **2000**, *69* (1−3), 59−86.

(2) Lambert, S. J. Geochemistry of the Waste Isolation Pilot Plant (WIPP) Site, Southeastern New Mexico, U.S.A. *Appl. Geochem.* **1992**, *7*, 513−531.

(3) Lambert, S. J.; Harvey, D. M. *Stable-Isotope Geochemistry of Groundwaters in the Delaware Basin of Southeastern New Mexico*; Sandia National Laboratories: Albuquerque, NM, 1987; pp 1−218.

(4) Lowenstein, T. K. Origin of Depositional Cycles in a Permian "Saline Giant": The Salado (McNutt Zone) Evaporites of New Mexico and Texas. *Geol. Soc. Am. Bull.* **1988**, *100* (4), 592−608.

(5) IAEA. *Status and Trends in Spent Fuel and Radioactive Waste Management.*; International Atomic Energy Agency: Vienna, Austria, 2018.

(6) Leigh, C.; Hansen, F. *Salt Disposal of Heat-Generating Nuclear Waste*; OSTI, 2011; p 1005078.

(7) Mackinnon, R.; Sevougian, S.; Leigh, C.; Hansen, F. *Towards a Defensible Safety Case for Deep Geologic Disposal of DOE HLW and DOE SNF in Bedded Salt*; OSTI, 2012; p 1057258.

(8) *The Disposal of Radioactive Waste on Land*; The National Academies Press: Washington, DC, 1957.

(9) *Used Fuel Disposition Campaign Disposal Research and Development Roadmap*; Argonne National Laboratory: Lemont, IL, 2012. Used Fuel Disposition Campaign (UFD Campaign).

(10) Kuhlman, K. L.; Sevougian, S. D. *Establishing the Technical Basis for Disposal of Heat-Generating Waste in Salt*; Sandia National Laboratories: Albuquerque, NM, 2013.

(11) Guiltinan, E. J.; Kuhlman, K. L.; Rutqvist, J.; Hu, M.; Boukhalfa, H.; Mills, M.; Otto, S.; Weaver, D. J.; Dozier, B.; Stauffer, P. H. Temperature Response and Brine Availability to Heated Boreholes in Bedded Salt. *Vadose Zone J.* **2020**, *19* (1), No. e20019.

(12) Roedder, E. The Fluids in Salt. *Am. Mineral.* **1984**, *69* (5−6), 413−439.

(13) Kuhlman, K.; Otto, S.; Stauffer, P.; Wu, Y. *Brine Availability Test in Salt (BATS) Extended Plan for Experiments at the Waste Isolation Pilot Plant (WIPP)*; OSTI, 2021; p 695014.

(14) Kuhlman, K. L.; Bartol, J.; Benbow, S. J.; Bourret, M.; Czaikowski, O.; Guiltinan, E.; Jantschik, K.; Jayne, R.; Norris, S.; Rutqvist, J.; Shao, H.; Stauffer, P. H.; Tounsi, H.; Watson, C. Synthesis of Results for Brine Availability Test in Salt (BATS) DECOVALEX-2023 Task E. *Geomech. Energy Environ.* **2024**, *39*, No. 100581.
(15) Craig, H. Isotopic Composition and Origin of the Red Sea and Salton Sea Geothermal Brines. *Science* **1966**, *154* (3756), 1544−1548.
(16) Craig, H. Isotopic Variations in Meteoric Waters. *Science* **1961**, *133* (3465), 1702−1703.
(17) Craig, H.; Gordon, L. I. Deuterium and Oxygen 18 Variations in the Ocean and the Marine Atmosphere. *Stable Isot. Oceanogr. Stud. Paleotemp.* **1965**, 9−130.
(18) Epstein, S.; Mayeda, T. Variation of O18 Content of Waters from Natural Sources. *Geochim. Cosmochim. Acta* **1953**, *4* (5), 213−224.
(19) Friedman, I. Deuterium Content of Natural Waters and Other Substances. *Geochim. Cosmochim. Acta* **1953**, *4* (1), 89−103.
(20) Bowen, G. J.; Cai, Z.; Fiorella, R. P.; Putman, A. L. Isotopes in the Water Cycle: Regional- to Global-Scale Patterns and Applications. *Annu. Rev. Earth Planet. Sci.* **2019**, *47*, 453−479.
(21) Bowen, G. J.; Cerling, T. E.; Ehleringer, J. R. Stable Isotopes and Human Water Resources: Signals of Change. In *Terrestrial Ecology*; Elsevier, 2007; Vol. *1*, pp 283−300.
(22) Galewsky, J.; Steen-Larsen, H. C.; Field, R. D.; Worden, J.; Risi, C.; Schneider, M. Stable Isotopes in Atmospheric Water Vapor and Applications to the Hydrologic Cycle. *Rev. Geophys.* **2016**, *54* (4), 809−865.
(23) Aron, P. G.; Levin, N. E.; Beverly, E. J.; Huth, T. E.; Passey, B. H.; Pelletier, E. M.; Poulsen, C. J.; Winkelstern, I. Z.; Yarian, D. A. Triple Oxygen Isotopes in the Water Cycle. *Chem. Geol.* **2021**, *565*, No. 120026.
(24) Knauth, L. P.; Beeunas, M. A. Isotope Geochemistry of Fluid Inclusions in Permian Halite with Implications for the Isotopic History of Ocean Water and the Origin of Saline Formation Waters. *Geochim. Cosmochim. Acta* **1986**, *50* (3), 419−433.
(25) O'Neil, J. R.; Johnson, C. M.; White, L. D.; Roedder, E. The Origin of Fluids in the Salt Beds of the Delaware Basin, New Mexico and Texas. *Appl. Geochem.* **1986**, *1* (2), 265−271.
(26) Bigeleisen, J.; Perlman, M. L.; Prosser, H. C. Conversion of Hydrogenic Materials to Hydrogen for Isotopic Analysis. *Anal. Chem.* **1952**, *24* (8), 1356−1357.
(27) Horita, J.; Ueda, A.; Mizukami, K.; Takatori, I. Automatic δD and δ18O Analyses of Multi-Water Samples Using H2- and CO2-Water Equilibration Methods with a Common Equilibration Set-Up. *Int. J. Radiat. Appl. Instrum., Part A* **1989**, *40* (9), 801−805.
(28) Coplen, T. B.; Wassenaar, L. I. LIMS for Lasers 2015 for Achieving Long-Term Accuracy and Precision of δ^{2}H, δ^{17}O, and δ^{18}O of Waters Using Laser Absorption Spectrometry: LIMS for Lasers 2015. *Rapid Commun. Mass Spectrom.* **2015**, *29* (22), 2122−2130.
(29) Gröning, M. Improved Water δ^{2}H and δ^{18}O Calibration and Calculation of Measurement Uncertainty Using a Simple Software Tool: Spreadsheet Calibration Strategy for Water Stable Isotopes. *Rapid Commun. Mass Spectrom.* **2011**, *25* (19), 2711−2720.
(30) Guidotti, S.; Jansen, H. G.; Aerts-Bijma, A. T.; Verstappen-Dumoulin, B. M. A. A.; van Dijk, G.; Meijer, H. A. J. Doubly Labelled Water Analysis: Preparation, Memory Correction, Calibration and Quality Assurance for δ^{2}H and δ^{18}O Measurements over Four Orders of Magnitudes: DLW δ^{2}H and δ^{18}O Measurements over Four Orders of Magnitudes. *Rapid Commun. Mass Spectrom.* **2013**, *27* (9), 1055−1066.
(31) Gupta, P.; Noone, D.; Galewsky, J.; Sweeney, C.; Vaughn, B. H. Demonstration of High-Precision Continuous Measurements of Water Vapor Isotopologues in Laboratory and Remote Field Deployments Using Wavelength-Scanned Cavity Ring-down Spectroscopy (WS-CRDS) Technology. *Rapid Commun. Mass Spectrom.* **2009**, *23* (16), 2534−2542.
(32) Uemura, R.; Nakamoto, M.; Asami, R.; Mishima, S.; Gibo, M.; Masaka, K.; Jin-Ping, C.; Wu, C.-C.; Chang, Y.-W.; Shen, C.-C. Precise Oxygen and Hydrogen Isotope Determination in Nanoliter Quantities of Speleothem Inclusion Water by Cavity Ring-down Spectroscopic Techniques. *Geochim. Cosmochim. Acta* **2016**, *172*, 159−176.
(33) van Geldern, R.; Barth, J. A. C. Optimization of Instrument Setup and Post-Run Corrections for Oxygen and Hydrogen Stable Isotope Measurements of Water by Isotope Ratio Infrared Spectroscopy (IRIS): Water Stable Isotope Analysis with IRIS. *Limnol. Oceanogr.: Methods* **2012**, *10* (12), 1024−1036.
(34) Dublyansky, Y. V.; Spötl, C. Hydrogen and Oxygen Isotopes of Water from Inclusions in Minerals: Design of a New Crushing System and on-Line Continuous-Flow Isotope Ratio Mass Spectrometric Analysis. *Rapid Commun. Mass Spectrom.* **2009**, *23* (17), 2605−2613.
(35) Affolter, S.; Fleitmann, D.; Leuenberger, M. New Online Method for Water Isotope Analysis of Speleothem Fluid Inclusions Using Laser Absorption Spectroscopy (WS-CRDS. *Clim. Past* **2014**, *10* (4), 1291−1304.
(36) Dassié, E. P.; Genty, D.; Noret, A.; Mangenot, X.; Massault, M.; Lebas, N.; Duhamel, M.; Bonifacie, M.; Gasparrini, M.; Minster, B.; Michelot, J.-L. A Newly Designed Analytical Line to Examine Fluid Inclusion Isotopic Compositions in a Variety of Carbonate Samples. *Geochem. Geophys. Geosyst.* **2018**, *19* (4), 1107−1122.
(37) de Graaf, S.; Vonhof, H. B.; Levy, E. J.; Markowska, M.; Haug, G. H. Isotope Ratio Infrared Spectroscopy Analysis of Water Samples without Memory Effects. *Rapid Commun. Mass Spectrom.* **2021**, *35* (8), No. e9055.
(38) de Graaf, S.; Vonhof, H. B.; Weissbach, T.; Wassenburg, J. A.; Levy, E. J.; Kluge, T.; Haug, G. H. A Comparison of Isotope Ratio Mass Spectrometry and Cavity Ring-down Spectroscopy Techniques for Isotope Analysis of Fluid Inclusion Water. *Rapid Commun. Mass Spectrom.* **2020**, *34* (16), No. e8837.
(39) Qi, H.; Coplen, T. B.; Tarbox, L.; Lorenz, J. M.; Scholl, M. USGS48 Puerto Rico Precipitation − a New Isotopic Reference Material for δ2H and δ18O Measurements of Water. *Isot. Environ. Health Stud.* **2014**, *50* (4), 442−447.
(40) Qi, H.; Lorenz, J. M.; Coplen, T. B.; Tarbox, L.; Mayer, B.; Taylor, S. Lake Louise Water (USGS47): A New Isotopic Reference Water for Stable Hydrogen and Oxygen Isotope Measurements. *Rapid Commun. Mass Spectrom.* **2014**, *28* (4), 351−354.
(41) Skrzypek, G.; Ford, D. Stable Isotope Analysis of Saline Water Samples on a Cavity Ring-down Spectroscopy Instrument. *Environ. Sci. Technol.* **2014**, *48* (5), 2827−2834.
(42) Stein, C. L.; Krumhansl, J. L. A Model for the Evolution of Brines in Salt from the Lower Salado Formation, Southeastern New Mexico. *Geochim. Cosmochim. Acta* **1988**, *52* (5), 1037−1046.
(43) Horita, J.; Friedman, T. J.; Lazar, B.; Holland, H. D. The Composition of Permian Seawater. *Geochim. Cosmochim. Acta* **1991**, *55* (2), 417−432.
(44) Lambert, S. J. *Fossil Meteoric Groundwaters in the Delaware Basin of Southeastern New Mexico*; Sandia National Laboratories: Albuquerque, NM, 1992; pp 1−44.
(45) Lambert, S. J. Geochemistry of Delaware Basin Ground Waters. *N. M., Bur. Mines Miner. Resour., Circ.* **1978**, *159*, 33−38.
(46) Hazen, R. M.; Roedder, E. How Old Are Bacteria from the Permian Age? *Nature* **2001**, *411* (6834), 155−155.
(47) Long, L. E.; Erwin, M. E.; Fisher, R. S. Rb-Sr Ages of Diagenesis of Mg-Rich Clay in Permian Sediments, Palo Duro Basin, Texas Panhandle, U.S.A. *J. Sediment. Res.* **1997**, *67* (1), 225−234.
(48) Renne, P. R.; Sharp, W. D.; Montañez, I. P.; Becker, T. A.; Zierenberg, R. A. 40Ar/39Ar Dating of Late Permian Evaporites, Southeastern New Mexico, USA. *Earth Planet. Sci. Lett.* **2001**, *193* (3), 539−547.
(49) Burgess, S. D.; Bowring, S.; Shen, Z. Q. High-Precision Timeline for Earth's Most Severe Extinction. *Proc. Natl. Acad. Sci. U.S.A.* **2014**, *111*, 3316−3321.
(50) Gonfiantini, R.; Wassenaar, L. I.; Araguas-Araguas, L.; Aggarwal, P. K. A Unified Craig-Gordon Isotope Model of Stable

https://doi.org/10.1021/acsearthspacechem.4c00107
ACS Earth Space Chem. XXXX, XXX, XXX−XXX

Hydrogen and Oxygen Isotope Fractionation during Fresh or Saltwater Evaporation. *Geochim. Cosmochim. Acta* **2018**, *235*, 224−236.
(51) Horita, J.; Wesolowski, D. J. Liquid-Vapor Fractionation of Oxygen and Hydrogen Isotopes of Water from the Freezing to the Critical Temperature. *Geochim. Cosmochim. Acta* **1994**, *58* (16), 3425−3437.
(52) McCaffrey, M. A.; Lazar, B.; Holland, H. D. The Evaporation Path of Seawater and the Coprecipitation of Br- and K+ with Halite. *SEPM J. Sediment. Res.* **1987**, *57*, 928−937.
(53) Gázquez, F.; Evans, N. P.; Hodell, D. A. Precise and Accurate Isotope Fractionation Factors (α17O, α18O and αD) for Water and CaSO4·2H2O (Gypsum). *Geochim. Cosmochim. Acta* **2017**, *198*, 259−270.
(54) Horita, J. Stable Isotope Fractionation Factors of Water in Hydrated Saline Mineral-Brine Systems. *Earth Planet. Sci. Lett.* **1989**, *95* (1−2), 173−179.

https://doi.org/10.1021/acsearthspacechem.4c00107
ACS Earth Space Chem. XXXX, XXX, XXX−XXX